Engineering Fracture Mechanics 148 (2015) 180–191

Contents lists available at ScienceDirect

Engineering Fracture Mechanics

journal homepage: www.elsevier.com/locate/engfracmech

Analysis of size and temperature effects in the ductile to brittle transition region of ferritic steels

C. Berejnoi [a,*], J.E. Perez Ipiña [b]

[a] Facultad de Ingeniería, Universidad Nacional de Salta, Avda. Bolivia 5150, 4400 Salta, Argentina
[b] CONICET/Facultad de Ingeniería, Universidad Nacional del Comahue, Avda. Buenos Aires 1400, 8300 Neuquén, Argentina

ARTICLE INFO

Article history:
Received 27 December 2014
Received in revised form 17 September 2015
Accepted 18 September 2015
Available online 26 September 2015

Keywords:
Ductile-to-brittle transition
Weibull distribution
Master Curve

ABSTRACT

This paper presents an analysis of ferritic steels in the ductile-to-brittle transition region that includes the determination of the temperature reference of the Master Curve, which assumes a Weibull distribution with fixed threshold and shape parameters for compact specimens of one inch thickness. Some differences arise between the scale parameter and the median of the distribution calculated from these specimens and those converted from other sizes. The dependence with size and temperature of the parameters of a non-fixed three parameter Weibull distribution were also analyzed. The estimated threshold and shape parameters resulted clearly temperature dependent, and different from those stated in the Master Curve.

1. Introduction

The characterization of fracture resistance of ferritic steels in the ductile-to-brittle transition region is problematic due to scatter in results, as well as size and temperature dependences.

Ferritic steels are, as defined in ASTM E1921-13 [1], "*typically carbon, low-alloy, and higher alloy grades. Typical microstructures are bainite, tempered bainite, tempered martensite, and ferrite and pearlite. All ferritic steels have body centered cubic crystal structures that display ductile-to-cleavage transition temperature fracture toughness characteristics*."

The statistical treatment is mainly based on Weibull statistics, which has been used with two (2P-W) (Eq. (1)) or three parameter (3P-W) (Eq. (2)). The parameters to be determined in the 2P-W distribution are the shape parameter, also known as Weibull slope (b_K or b_J), and the scale parameter (K_0 or J_0). For a 3P-W distribution, the threshold parameter (K_{min} or J_{min}) is added.

$$P = 1 - \exp\left[-\left(\frac{Jc}{J_0}\right)^{b_J}\right] \quad P = 1 - \exp\left[-\left(\frac{K_{Jc}}{K_0}\right)^{b_K}\right] \tag{1}$$

$$P = 1 - \exp\left[-\left(\frac{Jc - J_{min}}{J_0 - J_{min}}\right)^{b_J}\right] \quad P = 1 - \exp\left[-\left(\frac{K_{Jc} - K_{min}}{K_0 - K_{min}}\right)^{b_K}\right] \tag{2}$$

Data expressed in terms of K are derived from J_C (K_{JC}) using Eq. (3).

* Corresponding author. Tel.: +54 387 4255420.
E-mail addresses: berejnoi@unsa.edu.ar (C. Berejnoi), juan.perezipina@fain.uncoma.edu.ar (J.E. Perez Ipiña).

http://dx.doi.org/10.1016/j.engfracmech.2015.09.041
0013-7944/

Nomenclature

a_0	initial crack length
b_0	initial specimen remaining ligament
b_J	Weibull shape parameter estimated from J_C data
b_K	Weibull shape parameter estimated from K_{JC} data
$b_{k\text{-}1T}$	b_k for 1T-C(T) size (original and converted)
b_{Kj}	Weibull shape parameter derived from estimated b_J
r	number of non-censored tests
B	specimen thickness
B_{1T}	equivalent 1T-C(T) thickness
C(T)	compact tension specimen
E	elastic modulus
J_C	experimental J-integral at the onset of cleavage fracture
J_{max}	maximum allowed J_C value
J_{min}	Weibull threshold parameter estimated from J_C data
J_0	Weibull scale parameter estimated from J_C data
K_{J_c}	elastic–plastic equivalent stress intensity factor derived from the J_C value
$K_{Jc\text{-}1T}$	equivalent 1T-C(T) value of K_{J_c}
$K_{Jc(i)}$	*i-th* value of K_{J_c}
K_{Jmax}	maximum allowed K_{J_c} value
K_{med}	median of K_{J_c} distribution
K_{min}	Weibull threshold parameter
$K_{min\text{-}exp}$	minimum experimental K_{J_c}
$K_{min}(J)$	K_{min} derived from estimated J_{min}
$K_{min}(K)$	K_{min} estimated from K_{J_c} data
$K_{min\text{-}1T}$	K_{min} for 1T-C(T) size (original and converted)
K_0	Weibull scale parameter
$K_{0\text{-}1T}$	K_0 for 1T-C(T) size (original and converted)
$K_0(J)$	K_0 derived from estimated J_0
$K_0(K)$	K_0 estimated from K_{J_c} data
MC	Master Curve
N	total number of tests
T	test temperature
T_0	reference temperature
W	specimen width
ξ	factor relating b_J and b_{Kj}
ν	Poisson's ratio

$$K_{Jc} = \sqrt{\frac{EJ_c}{(1-\nu^2)}} \tag{3}$$

where E is the elastic modulus and ν is the Poisson's ratio.

For instance, Landes and Shaffer [2], Iwadate et al. [3], Anderson et al. [4], Landes et al. [5], and Heerens et al. [6,7] made use of a 2P-W distribution based on J_C values, while Landes and McCabe [8], Neville and Knott [9], and Perez Ipiña et al. [10] based their analysis on the 3P-W distribution using J_C data. The use of such distributions based on K values was promoted by Wallin, with a 2P-W distribution [11], and later with a 3P-W distribution [12].

Besides the possibility of working with two or three parameters, and also with J or K data, some authors have proposed a fixed shape parameter with a given value: 2 when working with J_C [4–6,13] and 4 when working with K_{JC} [1,12,14].

Although the 2P-Weibull slopes in terms of J and K are related by $b_K/b_J = 2$, this relationship does not apply when the third parameter (threshold parameter) is introduced. It was shown in previous papers [15,16] that the slopes ratio is not 2, and it is given by the factor $\xi = \frac{2K_0}{K_0+K_{min}}$. The slope b_{Kj}, converted from b_J using the factor $\triangleright$, and the b_K estimated from K_{Jc} values are not equals, but they are similar.

ASTM [1] has adopted the Master Curve method for the analysis of fracture toughness in this region. The temperature dependence of the 1T-C(T) median fracture toughness is based on an empirical equation calibrated at the T_0 temperature that corresponds to a $K_{med} = 100$ MPa m$^{0.5}$ for this size, and it is determined assuming a Weibull distribution with $K_{min} = 20$ MPa m$^{0.5}$ and slope $b_K = 4$ for the scatter treatment.

Prior to the Master Curve, ASME Boiler and Pressure Vessel Code already established the lower bound K_{IC} and K_{Ia} curves for the characterization of ferritic pressure vessel steels. The reference temperature was RT_{NDT} instead of T_0 [17]. Although the Master Curve method has represented a huge technological advance in the ductile-to-brittle transition region treatment introducing fracture toughness measurements and the effects of size and scatter, there are still some aspects that need a deeper analysis [18]. Neither the Weibull slope in terms of K is consistent with a fixed value equal to 4, nor the threshold value with 20 MPa $m^{0.5}$ [15], so the equation used in ASTM E1921 to model the specimen size effects would not work properly for toughness conversion from different specimen sizes other than 1 *in*. This work presents an analysis that includes the dependence of both T_0 and the calculated Weibull parameters ($K_0(J)$, $K_{min}(J)$ and b_{Kj}) and K_{med} with size and temperature.

2. Material and method

Data taken from the Euro Fracture Toughness Dataset [19] were used in the present work. They correspond to the Round Robin organized by the European Structural Integrity Society (ESIS) and all the information is available in ftp://ftp.gkss.de/pub/eurodataset.

The material tested in the project was a ferritic steel DIN 22NiMoCr37 forged, quenched and tempered. Tests were carried out at different temperatures (−154 °C, −91 °C, −60 °C, −40 °C, −20 °C, 0 °C and 20 °C) and with different specimen thicknesses C(T) (½″, 1″, 2″ and 4″, identified as 1/2T-C(T), 1T-C(T), 2T-C(T) and 4T-C(T) respectively), with a thickness to width ratio $B/W = 0.5$. Specimens were fatigue pre-cracked to be inside the range $0.52 < a_0/W < 0.6$. Side grooving was performed after pre-cracking in a few specimens. Tests were carried out in order to obtain the fracture toughness at the point of fracture, J_C.

Fig. 1 shows all the analyzed datasets for each temperature and size. Results are discriminated according to the type of fracture: cleavage without stable crack growth (✖), cleavage after some stable crack growth (■) and no cleavage (●). Also, the minimum experimental J value at each temperature (Min abs) and the allowed J_{max} (Max allowed) for each size are presented in Fig. 1. It is important to note that the "height" in the graphs of the different mechanisms for each size and temperature match the scatter presented, not the quantity of tests, and it corresponds mainly to cleavage results. For example, for 1/2T-CT and −20 °C over 31 tests, only 10 gave cleavage (✖ plus ■) and 21 gave no cleavage (●).

The discrimination presented in Fig. 1 was disposed in order to separate the effect of sets where two different failure modes coexist, implying that a 3P-W function could not adequately describe the scatter. It is important to note that some datasets with all the results corresponding to cleavage included also values greater than the allowed J_{max} for the corresponding thickness (1T-C(T) at −40 °C, 1T-C(T) at −20 °C and 2T-C(T) at 0 °C).

2.1. Master Curve parameters estimation procedure

T_0 values were calculated according to ASTM E1921 for all the Round Robin sets analyzed. This standard sets up a procedure for T_0 determination. It includes calculating the values of K_{J_c}, derived from Jc using Eq. (1) [1], the conversion of these last values to 1T-C(T) equivalent, as well as specifications for data censoring. In this work $E = 210$ GPa and $\nu = 0.3$ were used.

ASTM E1921 imposes two limits for K_{J_c} values: the first one is given by the condition of high crack-front constraint at fracture (Eq. (4)).

$$K_{Jmax} = \sqrt{\frac{Eb_0\sigma_{YS}}{30(1-\nu^2)}} \tag{4}$$

The second limit states that K_{Jc} values also shall be regarded as invalid for tests that terminate in cleavage after more than $0.05(W - a_0)$ or 1 mm (0.040 in.), whichever is smaller, of slow-stable crack growth.

The obtained K_{J_c} values for a B thickness specimen must be converted to 1T-C(T) equivalent by means of Eq. (5), resulting $K_{Jc\text{-}1T}$.

$$K_{Jc\text{-}1T} = K_{min} + [K_{Jc} - K_{min}] \cdot \left(\frac{B}{B_{1T}}\right)^{1/4} \tag{5}$$

where $K_{min} = 20$ MPa $\sqrt{m}$, and B_{1T} refers to the thickness of prediction (1T-C(T) specimen).

K_0 is calculated by means of Eq. (6):

$$K_0 = \left[\sum_{i=1}^{N} \frac{(K_{Jc(i)} - K_{min})^4}{r}\right]^{1/4} + K_{min} \tag{6}$$

$K_{Jc(i)}$ corresponds to the individual K_{J_c} (originally 1T-C(T) or converted to 1T-C(T) equivalent), r is the quantity of non-censored tests, and N the total number of tests.

Then K_{med} is calculated:

$$K_{med} = K_{min} + (K_0 - K_{min})[\ln(2)]^{1/4} \tag{7}$$

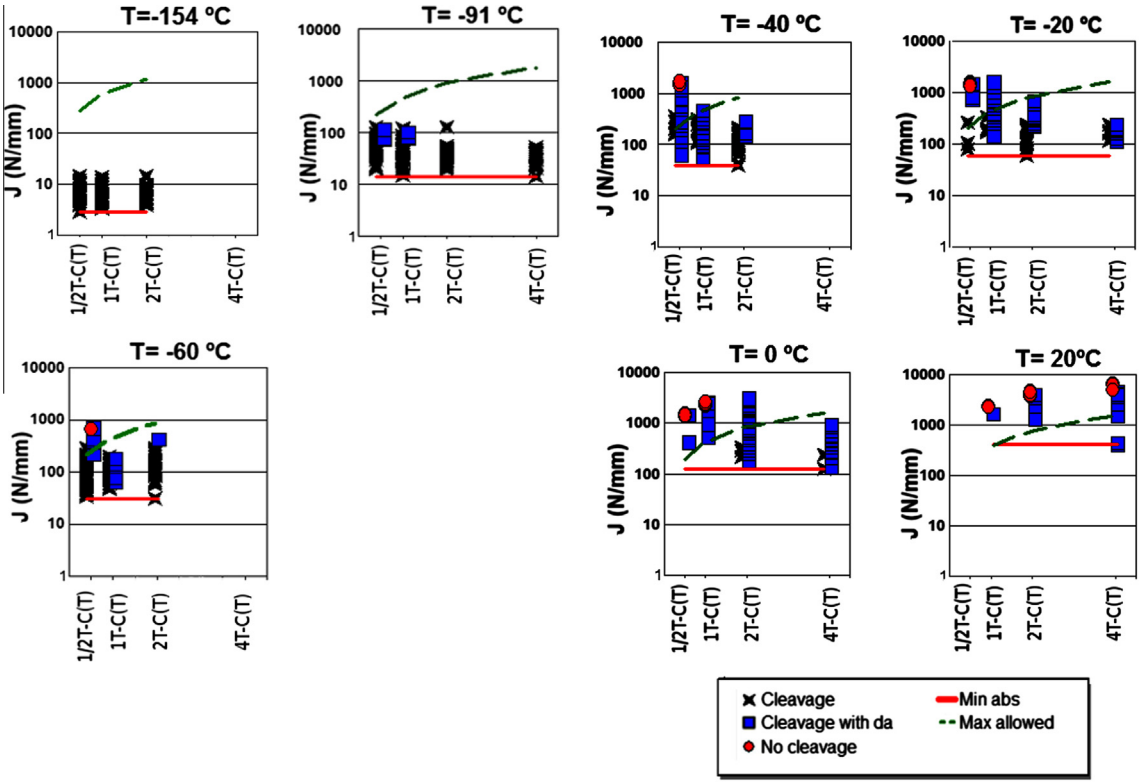

Fig. 1. Experimental results discriminated by type of fracture.

Considering K_{min} = 20 MPa m$^{0.5}$ and for a dataset tested at temperature T, the value of T_0 is obtained by means of Eq. (8).

$$T_0 = T - \left(\frac{1}{0.019}\right) \ln\left[\frac{K_{med} - 30}{70}\right] \tag{8}$$

The value 0.019 in Eq. (8), adopted by ASTM [1], was experimentally obtained using ferritic steels similar to the DIN 22NiMoCr37 tested in the Euro Round Robin [20,21].

In this work, the T_0 values were calculated at each temperature T using Eq. (8) for each series with data previously converted to 1T (Eq. (5)), and later more T_0 values were also obtained for a unique set composed by the total converted data for each temperature.

2.2. Estimation of K_{med} and 3P-W parameters b_{Kj}, $K_{min}(J)$, and $K_0(J)$

Distributions with parameters derived from the J estimation were employed because the $K_{min}(J)$ resulted less conservative than the $K_{min}(K)$ and were nearer to the experimental minimum [16].

The three parameter Weibull distribution presented in Eq. (3) was considered.

Working on Eq. (3), it results a linear relationship between $\ln(\ln(1-P)^{-1})$ and $\ln(J_c - J_{min})$ (Eq. (9))

$$\ln\left(\ln(1-P)^{-1}\right) = b_J \ln(J_c - J_{min}) - b_J \ln(J_0 - J_{min}) \tag{9}$$

J_{min}, J_0 and b_J were estimated for the same sets than T_0 by using the linear regression method. The most convenient J_{min} corresponds to the value that makes maximum the R^2 value of the regression, and then the other two parameters are calculated from the slope and ordinate of the linear function (Eq. (9)).

$K_{min}(J)$ and $K_0(J)$ were calculated by means of Eqs. (10) and (11), both based on the well-accepted relationship between K and J.

$$K_{min}(J) = \sqrt{\frac{EJ_{min}}{(1-\nu^2)}} \tag{10}$$

$$K_0(J) = \sqrt{\frac{EJ_0}{(1-\nu^2)}} \tag{11}$$

For b_{Kj} calculation, Eqs. (12) and (13) were used:

$$\xi = \frac{2K_0(J)}{K_0(J) + K_{min}(J)} \tag{12}$$

$$b_{Kj} = \xi \cdot b_J \tag{13}$$

The value of K_{med}, which corresponds to a probability of 0.5, was obtained using Eq. (14):

$$K_{med} = K_{min}(J) + (K_0(J) - K_{min}(J))(\ln 2)^{1/b_{Kj}} \tag{14}$$

3. Results, analysis and discussion

As expected, the general trend in experimental results is an increase in toughness as temperature increases, including median and experimental minimum values. As Fig. 1 clearly shows, the scatter is mainly consequence of cleavage failure (black + blue dots), non cleavage results give red[1] dots nearly superposed.

There is also a size effect but it depends on the crack growth mechanism. For cleavage, the general trend is that the scatter is larger for smaller specimens. Instead, some datasets corresponding to high temperatures and small sizes showed very low scatter because few or null cleavage results occurred. It is important to note that some datasets with 100% cleavage results included values greater than the allowed J_{max} for the corresponding thickness ((½ T-C(T) at −60 °C, 1T-C(T) at −40 °C, 1T-C(T) at −20 °C and 2T-C(T) at 0 °C).

The Weibull statistics describes scatter due to cleavage events and the results employed to obtain its parameters have to be valid as well. These two conditions make very difficult to obtain T_0 as well as to apply this methodology in the superior third of the ductile-to-brittle transition, especially for small specimens.

Out of the aforementioned, considering only valid cleavage results, neither the Weibull slope in terms of K is consistent with a fixed value equal to 4, nor the threshold parameter with a value of 20 MPa m$^{0.5}$ [16].

Consequently, the equation used in ASTM E1921 to model the specimen size effects would not work properly for toughness conversion from different specimen sizes other than 1 *in*.

3.1. Master Curve parameters computation

Table 1 shows T_0 values, as well as the difference between T_0 and the data set temperature for each dataset analyzed. The corresponding K_0 and K_{med} values are also shown. The results in parenthesis correspond to the values obtained after data censored according to ASTM E1921 [1]. Also, the number of specimen affecting the censoring is indicated.

Most censored data corresponded to the K_{Jmax} limit. Almost all the data that had to be eliminated by the ductile crack growth (Δa) limit were previously eliminated by K_{Jmax}. As Table 1 shows, censoring is larger for higher temperatures and smaller sizes. Only two data corresponding to 0 °C and B = 4T were censored just for Δa limit. Non-valid K_{J_c} began at −60 °C for 1/2T-C(T) specimens, while for 1T-C(T) they began at −40 °C, and for 2T-C(T) and 4T-C(T) they did not appear until 0 °C.

For 1/2T-C(T) and −40 °C most specimens were censored, although 8 valid results allowed a T_0 calculation. For this size and at higher temperatures, there were not enough valid (non censored) results to calculate a T_0 value.

For 1T-C(T) at −20 °C there were more than half non-valid results, although all of them presented cleavage. Instead, at 0 °C all the results were non-valid (only 7 cleavages), while at 20 °C only one specimen over 10 presented cleavage.

For 2T-C(T) and 4T-C(T) at 20 °C there were 9 and 12 cleavage tests over a total of 30 and 15 respectively, all non-valid for 2T-C(T) and only 2 valid results for 4T-C(T).

Fig. 2 shows the estimated T_0 values for the non-censored (a) and censored (b) conditions.

Comparing both graphs, the T_0 estimation shows less scatter when data are censored, giving support to the censoring procedure established in the standard.

The standard also states that the T_0 determination must be carried out with tests performed at temperatures near T_0, with a span lower than 50 °C. T_0 seems to be around −96 °C. Estimations shown in Fig. 2b exhibit a clear asymmetry: T_0 estimations from temperatures lower than T_0 and out of the admitted range, give very poor T_0 estimation (the standard does not allow testing at lower shelf regime), while for $T > T_0$, the limit imposed by the standard looks unnecessarily restrictive. Using the data censoring as the limit for high temperature seems to be more reasonable, although there will be more non-valid tests at higher temperatures and then more tests to be performed in order to reach the minimum number of valid results for T_0 calculation. All the sets corresponding to T = 20 °C, that gave bad T_0 estimations for non-censored data, were eliminated by lack of enough valid values when censoring was applied.

[1] For interpretation of color in Figs. 1 and 5–9, the reader is referred to the web version of this article.

Table 1
T_0, K_0 and K_{med}.

T (°C)	Size	Total tests	Cleavage tests	N_{NV}[a]	K_0 (MPa m$^{1/2}$)	K_{med} (MPa m$^{1/2}$)	T_0 (°C)	$T - T_0$ (°C)
−154	1/2T-C(T)	31	31	0	39.83	38.09	−40.42	−113.58
−154	1T-C(T)	34	34	0	42.43	40.46	−53.97	−100.03
−154	2T-C(T)	30	30	0	44.10	41.99	−61.13	−92.87
−154	All	95	95	0	42.30	40.35	−53.40	−100.6
−91	1/2T-C(T)	31	31	0	106.41	98.84	−90.12	−0.88
−91	1T-C(T)	34	34	0	116.11	107.7	−96.49	5.49
−91	2T-C(T)	30	30	0	117.05	108.55	−97.07	6.07
−91	4T-C(T)	15	15	0	117.25	108.73	−97.19	6.19
−91	All	110	110	0	114.12	105.88	−95.25	4.25
−60	1/2T-C(T)	31	31	2	146.59	135.51	−81.60	21.6
					(143.43)	(132.62)	(−80.13)	(20.13)
−60	1T-C(T)	34	34	0	158.63	146.5	−86.81	25.81
−60	2T-C(T)	30	30	0	229.77	211.41	−110.12	50.12
−60	All	95	95	2	189.61	174.76	−98.24	38.24
					(189.84)	(174.97)	(−98.32)	(38.32)
−40[b]	1/2T-C(T)	30	27	22	367.78	337.33	−117.86	77.86
−40	1T-C(T)	32	32	1	231.89	213.34	−90.68	50.68
					(232.15)	(213.58)	(−90.74)	(50.74)
−40	2T-C(T)	30	30	0	213.02	196.12	−85.48	45.48
−40	All	92	89	23	297.43	273.14	−105.53	65.53
					(223.42)	(205.61)	(−88.41)	(−48.41)
−20[b]	1/2T-C(T)	31	10	29	465.22	426.24	−111.24	91.24
−20	1T-C(T)	30	30	16	394.05	361.30	−101.82	81.82
					(340.55)	(312.48)	(−93.43)	(73.43)
−20	2T-C(T)	30	30	0	304.24	279.35	−86.86	66.86
−20	4T-C(T)	15	15	0	280.62	257.81	−82.11	62.11
−20	All	106	85	45	393.84	361.11	−101.79	81.79
					(309.22)	(283.9)	(−87.81)	(67.81)
0[b]	1/2T-C(T)	30	3	30	487.13	446.23	−93.83	93.83
0[b]	1T-C(T)	30	7	30	733.39	670.93	−116.55	116.55
0	2T-C(T)	30	30	12	656.28	600.57	−110.43	110.43
					(497.13)	(455.35)	(−94.99)	(94.99)
0	4T-C(T)	16	16	2	465.13	426.16	−91.23	91.23
					(475)	(435.16)	(−92.41)	(92.41)
0	All	106	56	74	630.70	577.23	−108.23	108.23
					(490)	(448.85)	(−93.16)	(93.16)
20[b]	1T-C(T)	10	1	10	725.05	663.32	−95.92	115.92
20[b]	2T-C(T)	30	9	30	1134.13	1036.58	−120.31	140.31
20[b]	4T-C(T)	15	12	13	1295.37	1183.71	−127.49	147.49
20[b]	All	55	22	53	952.44	870.80	−110.834	130.83

[a] N_{NV}: Number of specimen with $K_{J_c} > K_{Jmax}$ and/or violating Δa limitation.
[b] Corresponds to datasets where K_0 was unable to be calculated because the minimum number of valid results stated in the ASTM standard was not reached.

Fig. 3a and b shows K_0 values obtained using Eq. (4) at different temperatures and different specimen sizes, but with the K_{J_c} values previously converted to $K_{Jc\text{-}1T}$ equivalent by means of Eq. (5) with $K_{min} = 20\,\text{MPa}\sqrt{\text{m}}$. Each horizontal line corresponds to the value of K_0 when the original specimen size is 1T-C(T).

The general trend is that K_0 increases as T increases. For censored sets, K_0 appears not dependent of size. Instead, for non censored sets with several or all non-valid values, the calculated K_0 looks unrealistic. At high temperature and especially small sizes (1/2T-C(T) at and over −40 °C, 1T-C(T) at and over 0 °C and all sizes for 20 °C) there were not enough valid values to estimate K_0.

For each temperature, K_{med} was calculated for each size using Eq. (7), with K_0 given by Eq. (6) using censored data. In addition, the values of K_{med} were calculated for all the test results of different sizes at each temperature (converted to 1T-C(T) equivalent) taken as a unique dataset. Then, using Eq. (15) with T_0 = −96.5 °C, the K_{med} corresponding to the Master Curve was obtained.

$$K_{med} = 30 + 70\exp[0.019(T - T_0)] \tag{15}$$

Fig. 4 shows these results. For each temperature, the K_{med} value should be the same, independently of the original size, and it should also be located on the Master Curve. Fig. 4 shows that this almost verify for T = −154 °C and T = −91 °C, but it seems not to be valid for other cases. The Master Curve seems to slightly overestimate the K_{med} for −40 °C and −20 °C. The K_{med} values estimated for different sizes at equal temperature showed some scatter, especially for −60 and −20 °C, although no clear size tendency could be observed.

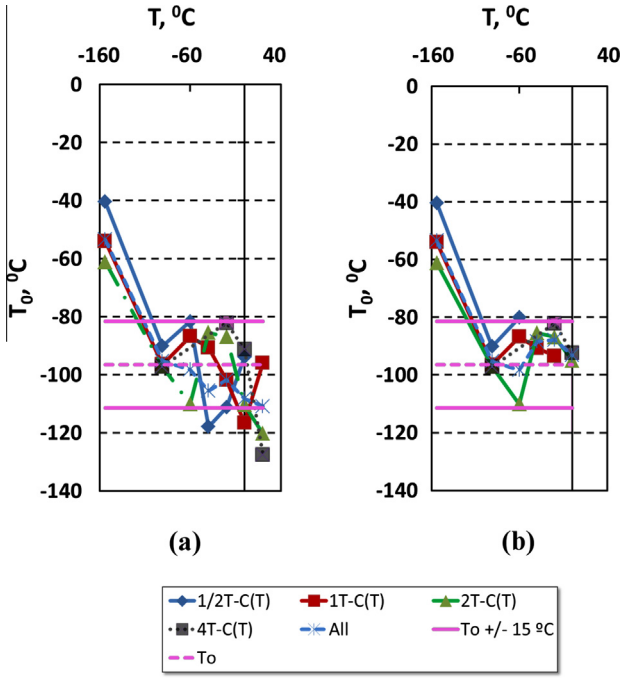

Fig. 2. T_0 according to ASTM E1921, at different temperatures and specimen sizes. (a) Non-censored data, (b) censored data.

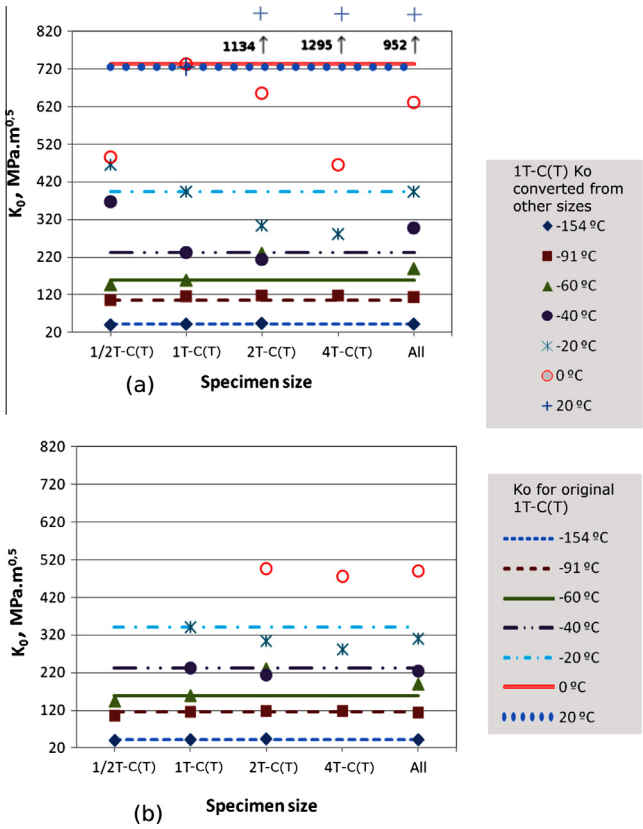

Fig. 3. K_0 according to ASTM E1921, at different temperatures and specimen sizes. (a) Non-censored data, (b) censored data.

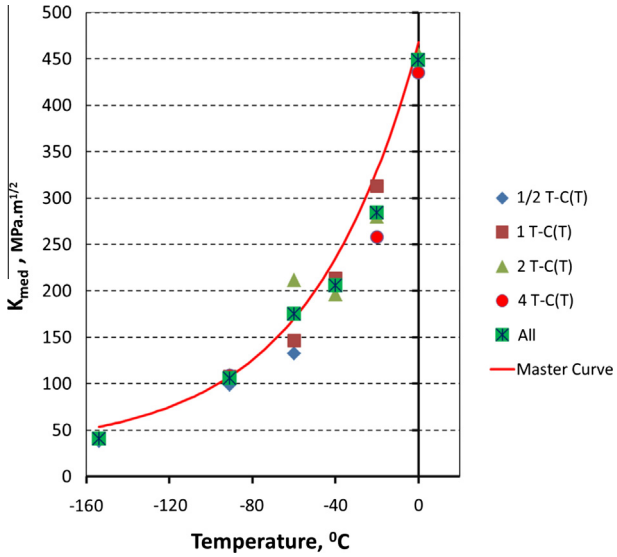

Fig. 4. K_{med} vs. T for different sizes and Master Curve according to ASTM E1921.

3.2. Analysis of 3P-W parameters

In this part, an analysis was performed using estimations from 3P-W functions without fixed parameters, instead of following ASTM E1921. Table 2 and Figs. 5–9 show the three-parameter values for the Weibull distribution, estimated using J_c values, and later converted to K equivalent parameters using Eqs. (10)–(13), and K_{med} calculated with Eq. (14). No data were converted to $K_{Jc\text{-}1T}$. The sets with censored values for the previous analysis are indicated in two groups: those with censored values are painted in yellow, while those with invalid sets for ASTM E1921 are painted in green.

In order to have a good description of experiments by means of a 3P-W function, at least three conditions must be fulfilled:

Table 2
Weibull parameters for different temperatures and sizes.

T (°C)	Size	$K_0(J)$ (MPa m$^{1/2}$)	K_{med} (MPa m$^{1/2}$)	$K_{min}(J)$ (MPa m$^{1/2}$)	b_{Kj}	K_{min}(experimental) (MPa m$^{1/2}$)
−154	1/2T-C(T)	42.76	40.2	20.41	3.01	25.42
−154	1T-C(T)	41	38.47	26.57	1.9	28.01
−154	2T-C(T)	38.16	36.18	29.1	1.49	29.61
−91	1/2T-C(T)	123.09	113.45	47.93	2.67	67.77
−91	1T-C(T)	113.35	102.98	52.27	1.97	58.64
−91	2T-C(T)	97.52	91.06	63.31	1.75	67.25
−91	4T-C(T)	90.54	85.3	30.65	4	56.43
−60	1/2T-C(T)	163.55	148.86	81.41	1.86	88.58
−60	1T-C(T)	157.23	145.89	97.5	1.74	103.81
−60	2T-C(T)	190.77	174.01	60.99	2.65	83.76
−40	1/2T-C(T)	379.81	322.14	107.5	1.54	119.23
−40	1T-C(T)	233.75	214.31	0	4.22	106.45
−40	2T-C(T)	182.6	169.78	72.14	2.97	96.08
−20	1/2T-C(T)	606.37	528.86	0	2.68	134.94
−20	1T-C(T)	361	318.9	170.21	1.47	179.1
−20	2T-C(T)	253.02	228.71	93.27	2.22	116.29
−20	4T-C(T)	209.92	201.36	116.14	3.83	160.77
0	1/2T-C(T)	618.67	584.24	0	6.4	307.37
0	1T-C(T)	781.16	734.87	0	6	343.47
0	2T-C(T)	469.1	396.16	195.92	1.18	200.56
0	4T-C(T)	325.34	291.49	136.97	1.85	170.86
20	1T-C(T)	747.11	729.1	0	15.02	615.55
20	2T-C(T)	997.66	950.93	0	7.64	543.87
20	4T-C(T)	913.47	793.37	0	2.6	305.71

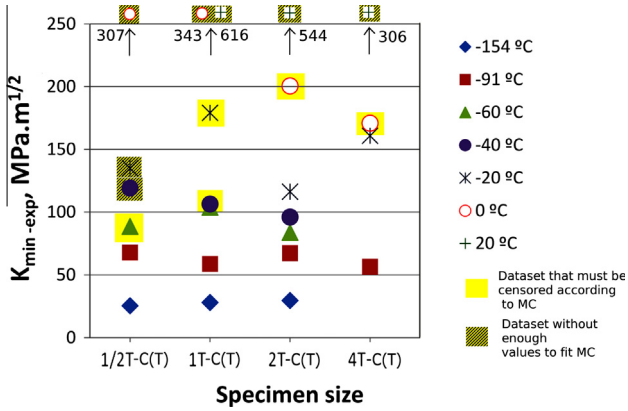

Fig. 5. K_{min} experimental as a function of specimen size and temperature.

- enough number of tests in the set to be representative of the population,
- all cleavage tests,
- valid J_c values.

Most sets are around 30 tests, which makes the first condition very probably fulfilled. Instead, the last two conditions are not satisfied for high temperatures and small specimens. This will give bad parameters estimations and is reflected also in the censoring methodology included in the Master Curve method.

The general tendency for the threshold parameter, K_{min}, is similar to the minimum experimental values, although with numerical values a little lower. As expected, their values increase as temperature increases and they did not show any tendency with size, for a given temperature. Instead, estimated K_{min} resulted null for 0 °C for the smaller sizes, and also for all sizes at 20 °C. The smaller sizes presented larger minimum experimental values than the larger ones for 0 °C and 20 °C, coinciding with all non-valid values for ASTM E1921 and most non-cleavage tests.

b_{Kj} values resulted close to 2 for sets of 1T-C(T) specimens with "valid" results. Only three sets showed values near 4 (4T-C(T) −91 °C; 4T-C(T) −20 °C; 1T-C(T) −40 °C, this last with just one cleavage non-valid value). There is not a clear tendency in b_{Kj} estimations with size and temperature.

Fig. 8 shows the effect of temperature and size in K_0. Considering only "valid" sets, the values of K_0 at constant thickness increase as temperature does and a soft tendency to decrease is shown with size increases while temperature remains constant.

Fig. 9 shows a similar trend for K_{med} calculated by means of Eq. (14), with that obtained by Eq. (7) as it is stated in ASTM standard [1].

The common denominator in this analysis is that for higher temperatures and smaller sizes the 3P-W parameters estimations are not good. This trend coincides with the occurrence of non-valid by censoring values given by ASTM E1921 and corresponds to no-cleavage values as well as to no valid cleavage results. It is necessary to introduce censoring, correction or another tool to avoid the influence of non-valid and non-cleavage tests.

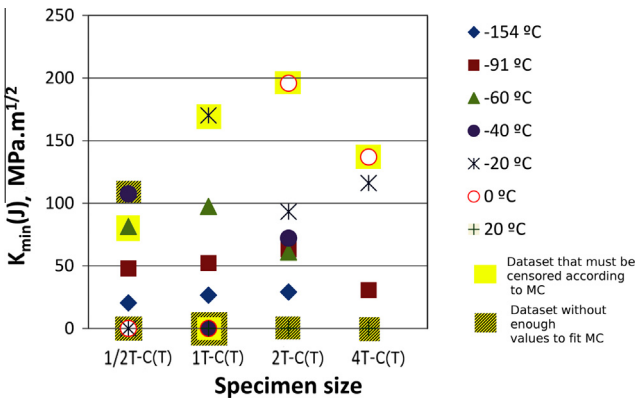

Fig. 6. K_{min} parameter as a function of specimen size and temperature.

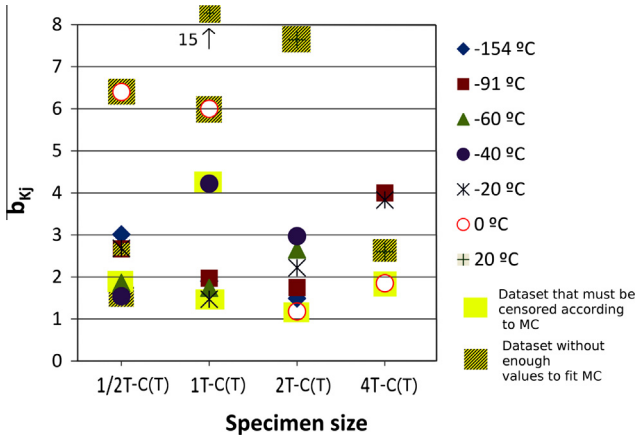

Fig. 7. b_{Kj} parameter as a function of specimen size and temperature.

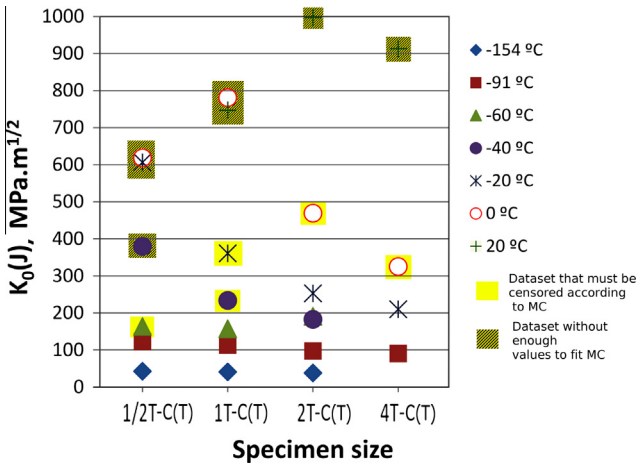

Fig. 8. K_0 parameter as a function of specimen size and temperature.

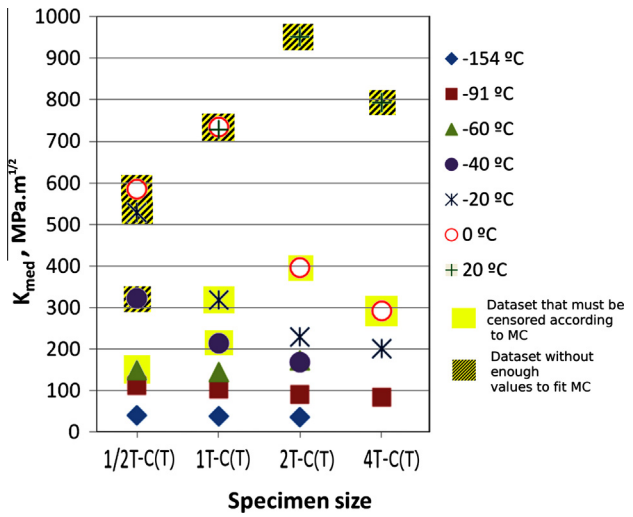

Fig. 9. K_{med} as a function of specimen size and temperature.

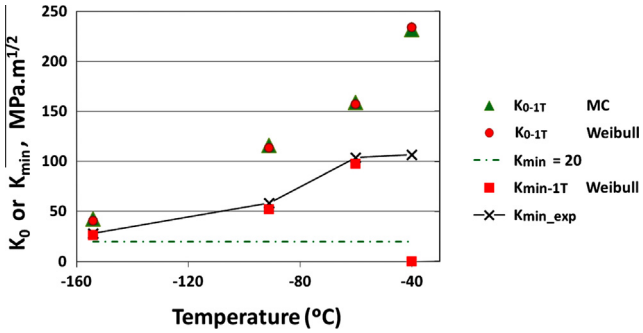

Fig. 10. $K_{0\text{-}1T}$ and $K_{min\text{-}1T}$ vs. temperature.

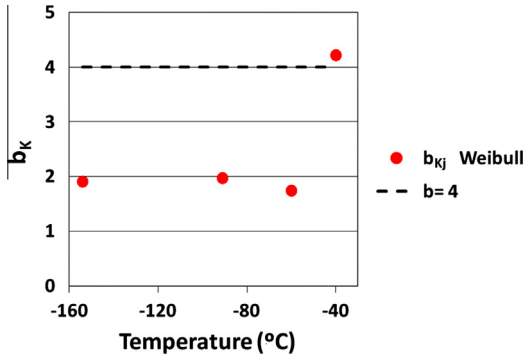

Fig. 11. $b_{k\text{-}1T}$ vs. temperature.

3.3. Comparison of 3P-W parameters with those given by the Master Curve method

In order to compare the estimation of $K_0(J)$, $K_{min}(J)$ and b_{Kj} using 3P-W distribution with the corresponding values of the Master Curve Method (K_0, K_{min} = 20 and b = 4), the datasets for 1T-C(T) specimens with all valid results (except −40 °C with only one censored datum) were used (Figs. 10 and 11). The values of $K_{0\text{-}1T}$ and $K_{min\text{-}1T}$ for Weibull correspond to $K_0(J)$ and $K_{min}(J)$ for 1T-C(T) size presented in Table 2, while the K_0 values corresponding to MC are cited in Table 1.

$K_{0\text{-}1T}$ for both Weibull and MC are quite similar, showing as expected, a tendency to increase with temperature. This occurs despite the fact that, in general, $K_{min\text{-}1T}$ and b_{Kj} for 3P-W are very different to the values of 20 MPa m$^{1/2}$ and 4 imposed by the MC method. The same occurs for K_{med} values for 1T-C(T) size that are calculated by Eqs. (7) and (14), and presented in Tables 1 and 2 for MC and Weibull, respectively.

From Fig. 10 it can be seen that the estimated $K_{min\text{-}1T}$ are much higher than 20, being lower than the experimental K_{min} for 1T-C(T) specimens, but close to them. Fig. 11 shows that the shape parameter b_{Kj} is close to 2. An exception to these observations is the dataset for T = −40 °C, which gives a $K_{min\text{-}1T}$ equal to zero and b_{Kj} near to 4. By the other hand, the Weibull slopes show a soft tendency to decrease as temperature increases, up to −40 °C. Slope values are lower than 4 as ASTM E1921 states.

The implementation of the Master Curve has been a huge advance in the need to have adequate tools for treating the complexities related to temperature, size and scatter in the ductile-to-brittle transition region for ferritic steels, but there are still some issues to be analyzed to enhance the reliability of the method without great conservatisms. This study showed that the hypothesis of constant slope and threshold can be very conservative, although the estimation of K_{med} is good.

4. Conclusions

- Master Curve analysis:
  Most of the analyzed sets provided a good prediction of T_0. The range of tolerance between the test temperature and T_0 appears to be asymmetric. As T gets near the lower shelf beginning, 50 °C of tolerance for $T < T_0$ might be too much. Instead, for $T > T_0$ this limit could be relaxed. Datasets with non-valid results gave inconsistent T_0 values, being necessary to implement data censoring. The equation used to convert data to 1T-C(T) equivalent size seems to work not well enough. If so, there will be no difference between the calculations of K_0 and K_{med} between original and equivalent 1T-C(T) size.

- 3P-W analysis:
  The use of small datasets does not allow a correct K_{min} and b_K estimation. But, in this work it is shown that the threshold parameter K_{min} and Weibull slope b_K are clearly dependent of temperature, and different from the values of 20 MPa $m^{0.5}$ and 4 considered in the Master Curve. This was found even for all valid data sets of 1T-C(T) size.
- Comparison between MC and 3P-W:
  When only valid datasets of 1T-C(T) size are considered, the values of K_0 and K_{med} obtained using a three-parameter Weibull distribution are in concordance with those obtained using ASTM E1921, although b_k and K_{min} were different. The fixed values stated in ASTM standard could not be appropriated when a size conversion criterion and/or some censoring procedure are included.

Acknowledgements

To Consejo Nacional de Investigaciones Científicas y Tecnológicas de Argentina (CONICET) and to Consejo de Investigación de la Universidad Nacional de Salta (CIUNSa) by the support to this work.

References

[1] ASTM E 1921-13. Standard test method for determination of reference temperature, T_0, for ferritic steels in the transition range. In: Annual book of ASTM standards 2013, vol. 03.01; 2013.
[2] Landes JD, Shaffer DH. Statistical characterization of fracture in the transition region. ASTM STP 700; 1980. p. 368–82.
[3] Iwadate T, Tanaka Y, Ono S, Watanabe J. An analysis of elastic–plastic fracture toughness behavior for J_IC measurement in the transition region. ASTM STP 803; 1983. p. 531–61.
[4] Anderson TL, Stienstra D, Dodds RH. A theoretical framework for addressing fracture in the ductile–brittle transition region. ASTM STP 1207; 1994. p. 186–214.
[5] Landes JD, Zerbst U, Heerens J, Petrovski B, Schwalbe KH. Single-specimen test analysis to determine lower-bound toughness in the transition. ASTM STP 1207; 1994. p. 171–85.
[6] Heerens J, Zerbst U, Schwalbe KH. Strategy for characterizing fracture toughness in the ductile to brittle transition regime. Fatigue Fract Engng Mater Struct 1993;16(11):1213–30.
[7] Heerens J, Pfuff M, Hellmann D, Zerbst U. The lower bound toughness procedure applied to the Euro fracture toughness dataset. Engng Fract Mech 2002;69:483–95.
[8] Landes JD, McCabe DE. Effect of section size on transition behavior of structural steels. Scientific paper 81-1D7-Metal-P2. Westinghouse R&D Centre; 1982.
[9] Neville D, Knott J. Statistical distributions of toughness and fracture stress for homogeneous and inhomogeneous materials. J Mech Phys Solids 1986;34(3):243–91.
[10] Perez Ipiña JE, Centurion SMC, Asta EP. Minimum number of specimens to characterize fracture toughness in the ductile-to-brittle transition region. Engng Fract Mech 1994;47(3):457–63.
[11] Wallin K. The scatter in K_{IC} – results. Engng Fract Mech 1984;19(6):1085–93.
[12] Wallin K. Statistical aspects of constraint with emphasis on testing and analysis of laboratory specimens in the transition region. ASTM STP 1171; 1993. p. 264–88.
[13] McCabe DE. A comparison of Weibull and $ß_{IC}$ analyses of transition range data. ASTM STP 1189; 1993. p. 80–94.
[14] Miglin M, Oberjohn L, Van Der Sluys W. Analysis of results from the MPC/JSPS Round Robin testing program in the ductile-to-brittle transition region. ASTM STP 1207; 1994. p. 342–54.
[15] Larrainzar C, Berejnoi C, Perez Ipina JE. Comparison of 3p-Weibull parameters based on J_c and K_{Jc} values. Fatigue Fract Engng Mater Struct 2010;34:408–22.
[16] Perez Ipiña JE, Berejnoi C. Experimental validation of the relationship between parameters of 3P-Weibull distributions based in J_C or K_{JC}. In: 13th International conference on fracture proceedings, Beijing, China; 2013. <http://www.icfweb.org/documents/proceedings/icf13-china-2013> [access in: 07.09.15].
[17] McCabe DE, Merkle JG, Wallin K. An introduction to the development and use of the Master Curve method. ASTM Stock Number: MNL52; 2005.
[18] Viehrig H-W, Zurbuchen C, Schindler H-J, Kalkhof D. Application of the Master Curve approach to fracture mechanics characterisation of reactor pressure vessel steel. Wissenschaftlich-Technische Berichte, Forschungszentrum Dresden FZD-536; 2010.
[19] Heerens J, Hellmann D. Development of the fracture toughness dataset. Engng Fract Mech 2002;69:421–49.
[20] Wallin K. Fracture toughness of engineering materials, estimation and application. EMAS: Publishing; 2011.
[21] Wallin K. The elusive temperature dependence of the Master Curve. In: 13th International conference on fracture proceedings, June 16–21, Beijing, China; 2013. <http://www.icfweb.org/documents/proceedings/icf13-china-2013> [access in: 07.09.15].